OPEN

In Vivo Risk Analysis of Pancreatic Cancer Through Optical Characterization of Duodenal Mucosa

Nikhil N. Mutyal, PhD, Andrew J. Radosevich, PhD,* Shailesh Bajaj, MD,† Vani Konda, MD,‡ Uzma D. Siddiqui, MD,‡ Irving Waxman, MD,‡ Michael J. Goldberg, MD,† Jeremy D. Rogers, PhD,* Bradley Gould, MS,* Adam Eshein, BS,* Sudeep Upadhye, MS,† Ann Koons, BS,‡ Mariano Gonzalez-Haba Ruiz, MD,‡ Hemant K. Roy, MD,§ and Vadim Backman, PhD**

Objectives: To reduce pancreatic cancer mortality, a paradigm shift in cancer screening is needed. Our group pioneered the use of low-coherence enhanced backscattering (LEBS) spectroscopy to predict the presence of pancreatic cancer by interrogating the duodenal mucosa. A previous ex vivo study (n = 203) demonstrated excellent diagnostic potential: sensitivity, 95%; specificity, 71%; and accuracy, 85%. The objective of the current case-control study was to evaluate this approach in vivo.

Methods: We developed a novel endoscope-compatible fiber-optic probe to measure LEBS in the periampullary duodenum of 41 patients undergoing upper endoscopy. This approach enables minimally invasive detection of the ultrastructural consequences of pancreatic field carcinogenesis.

Results: The LEBS parameters and optical properties were significantly altered in patients harboring adenocarcinomas (including early-stage) throughout the pancreas relative to healthy controls. Test performance characteristics were excellent with sensitivity = 78%, specificity = 85%, and accuracy = 81%. Moreover, the LEBS prediction rule was not confounded by patients' demographics.

Conclusion: We demonstrate the feasibility of in vivo measurement of histologically normal duodenal mucosa to predict the presence of adenocarcinoma throughout the pancreas. This represents the next step in establishing duodenal LEBS analysis as a prescreening technique that identifies clinically asymptomatic patients who are at elevated risk of PC.

Key Words: field carcinogenesis, pancreatic cancer, risk stratification, optical spectroscopy, low-coherence enhanced backscattering

(*Pancreas* 2015;44: 735–741)

Pancreatic cancer (PC) is the fourth leading cause of US cancer deaths and the most deadly with an overall 5-year survival of approximately 6% over the past decade.[1] One reason for such high mortality is that PC tends to develop surreptitiously over the course of multiple decades (ie, over 20 years from initiation to metastasis), with no appreciable symptoms presenting until the very final stages of cancer progression.[2] As a result, more than 50% of patients with PC are detected at a late time-point when distant metastases are present and there is a paltry 2% 5-year survival rate. Had these patients' condition been diagnosed while the disease remained localized to the pancreas, their survival rate would increase by more than 10 times. Whereas the insidious nature of PC is part of the reason that it is so lethal, it also means that there is a large window of time in which the precursors of frank cancer could be detected at a time-point long before it be comes terminal. To diagnose these more curable precursor lesions and lower the overall mortality of PC, a paradigm shift in which patients within the asymptomatic population are prescreened is needed.

One such alternative approach for PC detection exploits the concept of field carcinogenesis (ie, the earliest stage of cancer progression in essentially all solid cancers: pancreas,[3–6] colon,[7–9] lung,[10,11] head and neck,[12] etc) to assess the risk of a patient developing cancer. In field carcinogenesis, a number of ultrastructural alterations that are diffusely spread throughout an organ provide a fertile field from which future cancer development can proceed. By definition, these changes in tissue ultrastructure encompass all structures smaller than the diffraction limit of conventional light microscopy, or, structures smaller than approximately 200 nm. More advanced cancerous changes such as focal tumors and dysplasia can then take root in this field of ultrastructural alterations through stochastic mutational events such as up-regulation of oncogenes.

The implication of field carcinogenesis on cancer screening is as follows: Since changes in the field are found throughout an organ and nearby associated tissue locations, it is possible to gain an understanding of the organ cancer risk status through observation of easily accessible surrogate measurement locations. In the case of PC, most adenocarcinomas begin within the pancreatic duct. However, interrogating the pancreatic duct is not practical owing to the high risk of complications associated with such a procedure. Instead, the periampullary duodenum, which is exposed to the same milieu as the pancreatic duct (pancreatic juices and microbiome)[13] serves as a surrogate site from which cancer risk status can be assessed.

Unfortunately, none of the currently available diagnostic techniques are well suited for detecting the changes associated with PC field carcinogenesis. Widely used diagnostic imaging methods such as computed tomography, positron emission tomography, and magnetic resonance imaging can only detect larger lesions that occur at later stages of cancer progression. In addition, computed tomography and positron emission tomography use ionizing radiation that could create substantial adverse effects if implemented as populationwide screening techniques. Other endoscopic techniques that more directly interrogate the pancreas such as endoscopic ultrasound (EUS) and endoscopic retrograde cholangiopancreatography are also limited. Although EUS has increased

From the *Department of Biomedical Engineering, Northwestern University; †Department of Internal Medicine, NorthShore University HealthSystems, Evanston; ‡Center for Endoscopic Research and Therapeutics, University of Chicago Medicine, Chicago, IL; and §Department of Gastroenterology, Boston Medical Center, Boston, MA.

Received for publication June 9, 2014; accepted October 17, 2014.

Reprints: Hemant K. Roy, MD, Boston University Medical, 650 Albany St, Suite 526, Boston, MA 02118 (e-mail: hkroy@bu.edu).

This study was supported by National Institutes of Health grants R01CA128641, R01EB003682, R01CA156186, and U01CA111257. AJ Radosevich is supported by a National Science Foundation Graduate Research Fellowship under Grant No. DGE-0824162.

Drs. Roy, Goldberg, and Backman are cofounders/shareholders of American BioOptics LLC. Bradley Gould is a shareholder of American BioOptics LLC. The remaining authors declare no conflicts of interest.

Nikhil N. Mutyal and Andrew J. Radosevich contributed equally to this paper.

sensitivity to smaller lesions, it still does not allow detection of neoplastic lesions smaller than a few millimeters in size.[14] Endoscopic retrograde cholangiopancreatography is too invasive and expensive to be implemented as a populationwide screening technique.

To overcome the shortcomings of existing diagnostic technologies, our group has pioneered the use of low-coherence enhanced backscattering (LEBS) spectroscopy to detect the ultrastructural alterations associated with PC field carcinogenesis. Low-coherence enhanced backscattering uses nonionizing visible light spectroscopy to quantify tissue structures between approximately 30 nm and approximately 3 μm in size.[15] This range of sizes includes both the fundamental macromolecular building blocks of a cell (eg, mitochondria, ribosomes, and high-order chromatin structure) as well as components in the extracellular matrix (eg, collagen, elastin, fibronectons, etc).

In previous studies of ex vivo biopsies, we showed that LEBS could accurately discriminate between patients with no neoplasia and those harboring pancreatic adenocarcinomas by characterizing tissue from the periampullary duodenum (ie, tissue associated with field carcinogenesis).[3,4,16] Using a composite LEBS marker, the discrimination between healthy control patients and patients with PC had excellent diagnostic power with 95% sensitivity, 71% specificity, and 85% overall accuracy.[3] Furthermore, we demonstrated that this highly diagnostic signal originated in both intracellular and extracellular alterations (eg, chromatin density changes[17] and collagen fiber cross-linking[18]) occurring at structural length scales between approximately 20 and 200 nm in size. These changes were most prominent within the top approximately 150 μm of duodenal mucosa.[16,19] To translate our ex vivo findings to clinical practice, we developed a miniaturized fiber-optic probe to selectively target the upper 150-μm layer of mucosa in vivo.[20]

In this paper, we present a preliminary study of 41 patients as a proof of concept for the use of in vivo LEBS as a prescreening tool for PC. In this study, measurements from the periampullary duodenum are used as a surrogate site from which to assess PC risk status. Future directions and implications for the future of PC screening are summarized in the "Discussion" section.

MATERIALS AND METHODS

Participants

The study presented in this paper was approved by the institutional review boards at Northshore University HealthSystem and the University of Chicago Medical Center. Forty-one patients undergoing EUS or esophagogastroduodenoscopy to confirm the presence/absence of PC, mucinous cysts, pancreatitis, gallstones, etc. were recruited into the study after giving informed consent. All patients had available data taken from a complete endoscopic examination, from a pathology workup, and from a demographic information survey (age, race, smoking/alcohol status, personal and family history of cancer, etc). In total, 5 endoscopists at 2 medical institutions participated in the study.

Ten randomly spaced readings were acquired from the periampullary duodenal mucosa by a 3.4-mm diameter LEBS probe inserted through the accessory channel of an upper endoscope. Low-coherence enhanced backscattering measurements were performed by trained technicians, and the data analysis was performed by the investigators. Both the technicians and the investigators were blinded to the endoscopic and pathologic findings at the time of data acquisition and analysis. The investigators became unblinded only to perform statistical analysis. Based on the endoscopic and pathologic findings, patients were classified into 4 categories: no-neoplasia (control), pancreatitis (both acute and chronic), intraductal papillary mucinous neoplasia (IPMN), or pancreatic adenocarcinoma (PC). The presence of PC or IPMN was determined by fine needle aspiration (FNA) followed by histopathologic examination or imaging and surgery. Adenocarcinoma size, tumor stage, and location were estimated by an endoscopist and/or a pathologist.

Characterization of Tissue Ultrastructure Using LEBS

The principles underlying the characterization of tissue ultrastructure in PC field carcinogenesis have been described in great detail in other publications.[16,19] Here, we review the aspects relevant for the current paper.

The fundamental physical characteristic at the core of both tissue ultrastructure and light scattering detected by LEBS is the spatial autocorrelation function $B(r)$.[21,22] $B(r)$ specifies the range and proportion of all structural sizes that compose a particular specimen. For example, when $B(r)$ is very narrow, it means that the sample is primarily composed of smaller structures (and vice versa). In tissue composition, 3 ultrastructural properties specify the shape of $B(r)$: the fluctuation strength of spatial tissue heterogeneity σ_n^2, the characteristic structural length-scale L_n, and the shape of the spatial distribution D. Applying scattering theory and simple mathematical transformations,[23] the ultrastructural properties are directly related to the optical properties relevant for scattering: the reduced scattering coefficient μ_s^*, and the anisotropy factor g. These optical properties describe how light spreads throughout biological tissue owing to the effects of scattering.

Low-coherence enhanced backscattering is a coherent intensity peak centered at small backscattering angles (<3°) that arises owing to tissue heterogeneity. Through use of partial spatial coherence illumination, LEBS targets the short photon transport paths that preserve information about μ_s^*, g, and D.[24–27] To quantify LEBS data, we measured 3 empirical parameters that specify the shape of the LEBS peak: the height (termed enhancement E), width (W), and spectral slope (S, change in E per unit wavelength). These 3 empirical parameters can then be used to deduce the optical properties and physical properties, which better describe tissue structure.

In summary, nanoscale tissue composition is quantified by the ultrastructural properties σ_n^2, L_n, and D. The ultrastructural properties give rise to the optical properties μ_s^* and g. The optical properties determine the shape of the LEBS peak, which is quantified with empirical parameters E, W, and S.

Targeting The Ultrastructural Origins of Field Carcinogenesis In Vivo

In 2 recent publications, we analyzed duodenal biopsies using LEBS and inverse scattering optical coherence tomography to study the nature and location of the changes in tissue ultrastructure associated with PC field carcinogenesis.[16,19] Several key observations from these studies guided the design of the fiber-optic LEBS probe used in the current study. First, we measured a significant increase in D and a decrease in σ_n^2 for patients with PC. These ultrastructural changes combined to produce a significant decrease in μ_s^*. Second, we found that the optimal location to find such alterations was within the upper approximately 150 μm of mucosa. Finally, the changes were attributed to structures smaller than the diffraction limit of conventional light microscopy (ie, ~200 nm). Conventional endoscopic methods would be insufficient to detect the structural changes in PC field carcinogenesis.

Armed with these observations, we designed a fiber-optic probe capable of detecting the previously observed changes in D and μ_s^* occurring within the superficial duodenal mucosa.[20] The design and theoretical principles underlying the fiber-optic LEBS

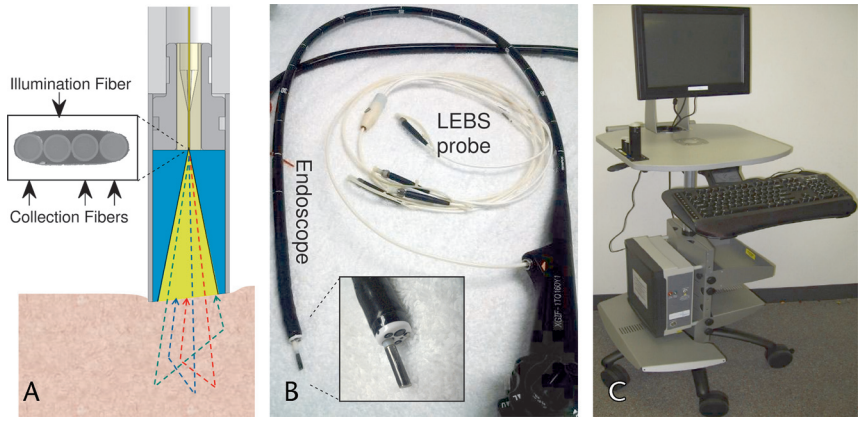

FIGURE 1. Clinical LEBS spectroscopy instrument design. A, Schematic of the 3.4-mm diameter fiber-optic LEBS probe. White light is directed onto the tissue by a single optical fiber. Three optical fibers collect the backscattered light as a function of angle and illumination wavelength. The inset shows a microscopic image of the linear optical fiber array. B, Low-coherence enhanced backscattering probe inserted into the accessory channel of an upper endoscope. The inset shows the LEBS probe extending from the endoscope. C, Portable cart used to house the data acquisition instrumentation and software for the LEBS probe.

probe are described in full in other publications.[20,28] In short, the LEBS probe consists of 4 optical fibers arranged in a linear array (shown in the inset of Fig. 1A). One of these fibers provides white light illumination onto the tissue surface, whereas the remaining 3 fibers acquire LEBS intensities at 3 backscattering angles: −0.6, 0.6, and 1.12 degrees. A 9-mm glass rod spacer is placed between the optical fibers and tissue surface to control the spatial coherence length L_{SC} of the illumination. Each collection fiber is connected to a spectrometer, which collects backscattered light as a function of wavelength (500–700 nm). Thus, the LEBS probe measures backscattered light as a function angle and wavelength. The choice of backscattering angle and wavelength was optimized to target the ultrastructural alterations in duodenal mucosa observed in previous ex vivo biopsy studies.[3,16] To target the upper 150 μm of duodenal mucosa where the optimal signal is observed, we restricted the spatial coherence length to 27 μm at 700-nm illumination wavelength.[20,29]

A schematic illustrating the operation of the LEBS probe (assembled by OFS, Avon, CT) is shown in Figure 1A. The outer diameter of the LEBS probe is 3.4 mm, which allows it to be inserted into the accessory channel of commercially available endoscopes (Fig. 1B). Patient measurements are then managed through a point-of-care optical system (assembled by Tricor Systems, Elgin, IL) with custom data acquisition software and instrumentation (Fig. 1C).

Two independent diagnostic parameters are calculated using the measured LEBS intensities: enhancement (E') and normalized spectral slope (NSS). The spectrally resolved $E'(\lambda)$ is calculated as the average of the intensities at −0.6 degree and +0.6 degree minus the intensity at 1.12 degree. E' is then found as the average of $E'(\lambda)$ over the wavelength range 610 to 690 nm. Normalized spectral slope is calculated in 2 steps. First, the spectral slope (S') of $E'(\lambda)$ is calculated using a linear regression of the form $E'(\lambda) = K - S'\lambda$ over the wavelength range 610 to 690 nm. To remove the contribution of E', NSS is calculated by dividing S' by E' and multiplying by the average wavelength: $NSS = -S' \times \frac{<\lambda>}{E'}$.

The parameters E' and NSS represent measurable quantities that encode information about tissue ultrastructure. However, to gain a more physical understanding of the tissue composition and target the previously observed alterations, we also calculated the physical/optical properties D and μ_s^*. To do this, we first made the assumption that $g = 0.9$ in biological tissue.[30] D and μ_s^* can then be found according to equations empirically derived from Monte Carlo simulation[31]: $D = 0.80 \times NSS + 2.85$ and $\mu_s^* = 3590\ \text{cm}^{-1} \times E' + 3010\ \text{cm}^{-1} \times E' \times NSS - 4.53\ \text{cm}^{-1}$. To achieve agreement between Monte Carlo simulation and experimentally measured intensities, the value of E' was multiplied by a constant scaling factor of 0.31. Possible origins of the discrepancy between theory and experiment are discussed in Radosevich et al.[26]

Statistical Analysis

The 2 parameters previously discussed were combined into a single diagnostic biomarker (termed the LEBS marker) using a multivariable logistic regression performed in STATA version 8.0. The final model was built as a linear combination of E' and NSS as follows:

$$\text{LEBS marker} = a_0 + a_1 \times E' + a_2 \times NSS \qquad 1$$

where a_0, a_1, and a_2 are coefficients assigned in STATA. The internal validity of the regression model was assessed using bootstrapping techniques. Under this approach, the shrinkage factor was obtained to correct for overoptimism or overfitting, and the regression coefficients were multiplied by this factor to improve calibration of prediction in future patients. The intercept was also adjusted so that the sum of the predicted probabilities equaled the total number of events.

The correlation coefficient between each of the selected parameters was verified to be nonsignificant ($R^2 < 0.3$) to ensure the robustness of the generated model. The prediction rule was developed to optimize the difference between control and PC.

To characterize the performance of the diagnostic test, we calculated the sensitivity, specificity, and the overall accuracy by generating the receiver operating characteristic (ROC) curve in STATA. Contributions of confounding factors (age, race, smoking/alcohol status, and personal and family history of cancer) toward the LEBS marker were evaluated by performing analysis of covariance.

RESULTS

Patients' Characteristics

Measurements from the periampullary duodenum were acquired from a total of 41 patients undergoing upper endoscopy (age, 61 ± 15 years; sex, 37% male; race, 98% white). The age,

TABLE 1. Patients' Demographics

Patient Category	Age (Mean ± SD)	Sex (% Male)	Race (% White)	No. Patients
Control	58 ± 17	25	95	20
Pancreatitis	55 ± 17	80	100	5
IPMN	70 ± 5	29	100	7
PC	63 ± 13	44	100	9

TABLE 2. Test Performance Characteristics

Comparison	Sensitivity (%)	Specificity (%)	AUC [95% CI]
Control vs PC	78	85	81% [64%–98%]
Control vs IPMN	86	55	71% [45%–97%]
Control vs pancreatitis	80	70	74% [54%–94%]

sex, and race for all patients separated according to their disease status are summarized in Table 1. Nine patients were diagnosed with pancreatic adenocarcinomas (PC), of which 7 were harboring lesions in the head/neck of the pancreas and 2 in the body/tail of the pancreas. Within the PC group, 4 patients had stage I or II cancer, and 5 patients had stage III or IV cancer. Of the 7 patients with IPMN, 4 were located in the side branch and 3 were located in the main duct. Five patients had either acute or chronic pancreatitis. Finally, 20 patients were healthy controls with no disease found in the pancreas.

Evaluation of the LEBS Marker in Duodenal Mucosa

Figure 2A shows the values of the LEBS marker for patients with increasing susceptibility to progress into PC from left to right. Qualitatively, there is a progressive increase in the LEBS marker for increasing disease status. Relative to the controls, this increase is highly statistically significant for PC, with $P < 0.01$; whereas for patients with IPMN, the effect is marginally significant, with $P = 0.08$. For pancreatitis versus control, the LEBS is not significant with $P = 0.23$. Taken together, these results show that the LEBS marker encodes information about increasing PC disease status.

Figure 2B shows the receiver operating characteristic (ROC) curves for control versus PC, control versus IPMN, and control versus pancreatitis. The LEBS marker provided good test performance characteristics with 81% overall accuracy (ie, area under the ROC curve) for distinguishing between control and PC. For detection of IPMN and pancreatitis, the test performance characteristics were respectable with 71% and 74% accuracy, respectively. The sensitivity, specificity, and accuracy for both PC and IPMN are summarized in Table 2.

Influence of Cancer Stage, Tumor Location, and IPMN Location

To further study the diagnostic potential of LEBS across different forms of PC, we separated the PC group according to cancer stage (Fig. 3A) and tumor location (Fig. 3B). For early lesions in cancer stages I and II, there is a significant increase in the LEBS marker; whereas for cancer stages III and IV, there is a nearly significant increase ($P = 0.07$). This is an encouraging result, since LEBS can detect the early-stage alterations needed for an effective prescreening technique. We expect that with a larger sample size, the later stage subgroup will also become significant. Comparing cancer stages I and II with cancer stages III and IV, the difference was nonsignificant with $P = 0.43$.

For lesions found in the head and the neck as well as the body and tail of the pancreas, there was a statistically significant increase in the LEBS marker with $P < 0.05$. Comparing lesions of the head and neck with those of the body and tail, the difference was nonsignificant, with $P = 0.11$.

Figure 3C decomposes the patients with IPMN according to the location in which the lesions were found. We found a significant increase for main duct IPMN but essentially no effect for side branch IPMN. This is likely because the main duct empties directly into the periampullary duodenum from which our LEBS measurements were acquired.

Potential Confounders

To determine the effect of confounding factors on our results, we performed an analysis of covariance with the LEBS

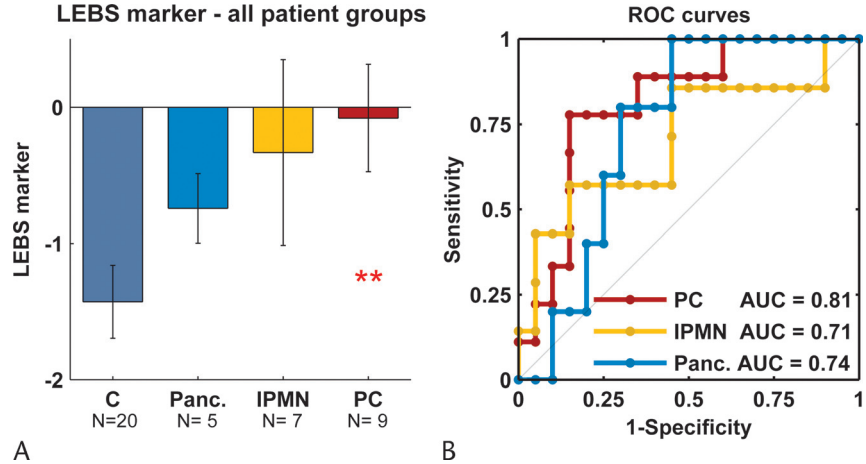

FIGURE 2. Diagnostic performance of the LEBS marker for patients with different risks of developing PC (increasing risk from left to right). A, Low-coherence enhanced backscattering marker calculated from a logistic regression of E' and NSS. B, Receiver operating characteristic curve for patients with PC and IPMN. The double red star indicates statistically significant difference from control at the 1% level. C, control; Panc, pancreatitis.

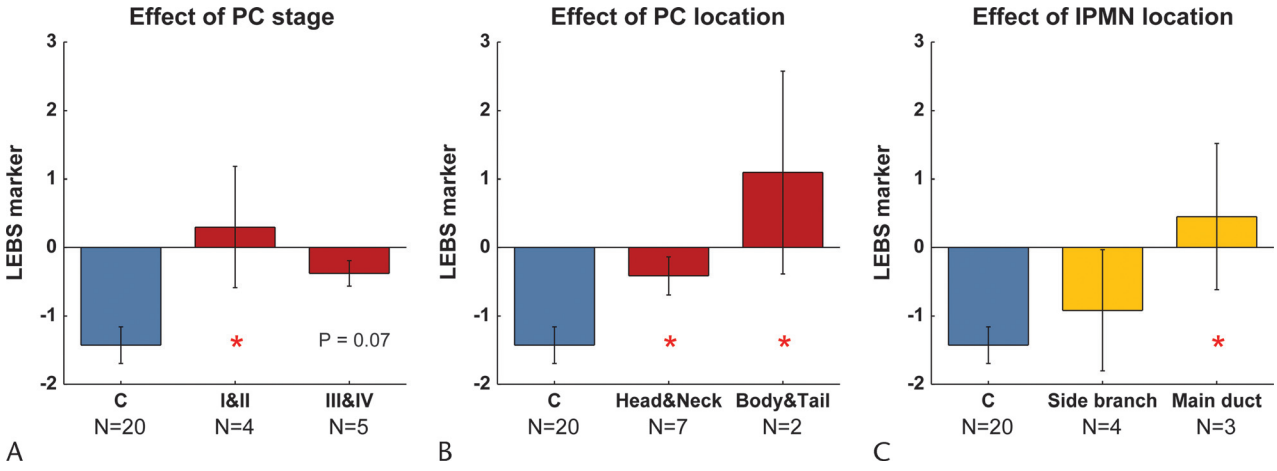

FIGURE 3. Influence of cancer stage, tumor location, and IPMN location on the diagnostic performance of LEBS. A, Influence of cancer stage. B, Influence of tumor location within the pancreas. C, Influence of IPMN location within the pancreas. In each panel, a red star indicates statistically significant difference from control at the 5% level.

marker as the dependent variable; and the presence of neoplasia, smoking and alcohol history, race, sex, age, personal and family history of cancer as predictors (Table 3). After incorporating these confounding factors into our model, the LEBS marker remained a highly significant predictor for the presence of neoplasia ($P = 0.02$). Moreover, each of the confounding factors was found to have an insignificant effect ($P > 0.05$) on the LEBS marker value.

Relating LEBS Marker to Optical Properties

Figure 4 shows the optical properties D and μ_s^* that were extracted from the empirical parameters, which form the LEBS marker. In Figure 4A, there is a highly significant 41% increase in D for patients with PC. The increase in D indicates a shift in tissue ultrastructure toward larger structures. In Figure 4B, there is a 39% decrease in μ_s^* for patients with PC ($P = 0.26$). Importantly, the directionality of these changes is consistent with 2 previous ex vivo biopsy studies.[3,16]

DISCUSSION

In this paper, we demonstrated the first in vivo implementation of the fiber-optic LEBS probe to discriminate patients with PC and IPMN from healthy controls through optical interrogation of the endoscopically normal-appearing periampullary duodenum. These results were obtained in a multicenter clinical trial consisting of 2 hospitals and 5 endoscopists. The current study provided an important confirmation that in vivo measurements detect the same alterations that were previously observed in ex vivo tissue (ie, D and μ_s^*).[16,19] Moreover, the diagnostic LEBS marker provided an excellent biomarker for detecting the susceptibility of patients toward developing PC. We saw a progressive increase in the value of the LEBS marker with a corresponding increase in patients' disease status (control < pancreatitis < IPMN < PC). Between the patients with PC and the healthy controls, the LEBS marker was highly significant ($P < 0.01$), resulting in an overall detection accuracy of 81%. This relationship was not confounded by race, age, sex, cancer history, or other lifestyle choices such as smoking and alcohol status. Furthermore, by separating the patients with PC into subgroups, we found that the diagnostic effects were present regardless of the lesion location. For the patients with PC in cancer stage I or II, we found a significant effect and for the patients in cancer stage III or IV, there was a nearly significant effect ($P = 0.07$). Finally, by decomposing the patients with IPMN according to their lesion location, we found that most of the effect was attributable to main duct IPMN.

From a mechanistic perspective, the change in D provides the best insight into the morphological changes occurring in the duodenum during PC field carcinogenesis. Whereas LEBS lacks the spatial resolution to identify the specific structures, which contribute to the observed change in D, there is evidence of synergistic intracellular (eg, nucleus, cytoskeleton, and mitochondria) and extracellular contributions (eg, collagen fibers), which account for this shift toward larger features. Within epithelial cells in field carcinogenesis, we have observed chromatin compaction in the nucleus induced, in part, by up-regulation of the histone deacetylase family of proteins (a class of enzymes that aids in histone wrapping).[17,18] We confirmed that the observed chromatin compaction resulted in an increase in D using direct visual confirmation with transmission electron microscopy.[32] In addition to changes in the nucleus, we also observed LEBS-detectable alterations of the cytoskeletal structure due to up-regulation of end-binding protein 1.[33,34] Within the extracellular matrix, the increase in D is attributed to collagen cross-linking initiated by the up-regulation of lysyl-oxidase or lysyl-oxidaselike proteins.[18] Interestingly, each of the changes that we observed in field carcinogenesis (ie, chromatin compaction, abnormal cytoskeleton, and collagen cross-linking) is also a traditional hallmark of later-stage cancer development. Whereas in the later cancer stages these changes manifest themselves in the larger structural length scales (microns to 10s of microns), in field carcinogenesis, they occur at ultrastructural length scales (10s of nanometers to hundreds of nanometers).

TABLE 3. Impact of Confounding Factors on the LEBS Marker

Confounding Factor	ANCOVA (P)
Presence of adenocarcinoma	0.02
Age	0.81
Sex	0.07
Smoking history	0.71
Alcohol use	0.79
Personal history of PC	0.08
Personal history of other cancer type	0.73
Family history of PC	0.17
Family history of other cancer type	0.47

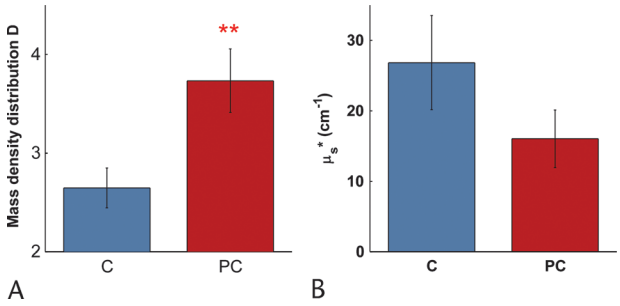

FIGURE 4. Optical properties extracted from *E* and NSS. A, Mass density distribution *D*. B, Reduced scattering coefficient μ_s^*. A double red star indicates statistically significant difference from control at the 1% level.

We note that the specific alterations previously discussed are only some of the many changes that occur in PC field carcinogenesis and should not be considered an exhaustive list. Ongoing mechanistic studies seek to further catalog all LEBS-relevant changes in tissue ultrastructure.

Despite the encouraging results, we acknowledge a number of limitations in the current study. First, the overall size of the data set is modest ($N = 41$) and is therefore more susceptible to statistical noise than a larger study. To address this concern, larger multicenter studies are currently underway. Nonetheless, we note that our use of only 2 uncorrelated parameters is conservative and limits the likelihood of overfitting the data. Second, the current study was composed primarily of white patients (>98%). It will therefore be important to study the application of this technique to demographically distinct populations to further establish external validity and promote widespread LEBS application. Similarly, patients with PC were slightly older than the healthy controls. Although age is not a confounding factor in our analysis, it will be important to study the application of this technique across a wider age span.

Despite the aforementioned limitations, the test performance characteristics of in vivo duodenal LEBS are very encouraging. Moreover, this performance may be further improved with additional biomarkers. For example, the LEBS fiber-optic probe is capable of measuring microvascular markers such as hemoglobin oxygen saturation and blood vessel radius.[35] In fact, we found some of the microvascular markers to have a moderate statistical significance for patients in our study (data not shown). However, we did not apply these markers to our prediction rule formulation to avoid overfitting of our modest data set. Still, in ongoing larger-scale studies, we expect that addition of these markers will lead to improved test performance characteristics.

From a clinical perspective, we envision the use of LEBS as the first step in 2-part paradigm shift in PC screening. This process would work in the following way: First, patients considered to be at risk of developing PC according to genetic factors (eg, family histories with high PancPro score, BRCA2 mutations, p16 mutations, Peutz-Jeghers, etc) or environmental/developed factors (new-onset diabetes after age 50, pancreatic cysts, chronic pancreatitis, and smoking) would have their specific risk status analyzed using LEBS coupled with ultrathin endoscopy to provide a pan–upper GI screening. This procedure is minimally invasive and would likely circumvent the major adverse complications that have been associated with direct interrogation of the pancreatic duct. Patients who are found to be at higher risk of PC can then undergo more invasive and costly techniques to confirm the presence of early PC lesions.

One main application of this clinical approach would specifically target cystic lesions of the pancreas such as IPMN. In approximately one third of all incidentally discovered pancreatic cysts undergoing surgical resection, the preoperative diagnosis was found to be incorrect retrospectively.[36] This inability to accurately risk-stratify cystic neoplasms leads to medical complications, a strain on resources (eg, extra procedures, biopsies, etc) and a great deal of patient anxiety due to the lethality of PC. The consequence has been that pancreatic resections have doubled over the last decade without a decrease in PC deaths. Based on the present findings, LEBS is a promising alternative method to assess the disease status of the pancreas in patients with cystic lesions. Those patients with cystic lesion with high-risk for PC would be recommended for EUS, endoscopic retrograde cholangiopancreatography, and/or surgery.

In summary, we showed for the first time the feasibility of in vivo measurement of histologically normal duodenal mucosa to predict the presence of adenocarcinoma throughout the pancreas. This represents the next step in establishing duodenal LEBS analysis as a prescreening technique that identifies clinically asymptomatic patients who are at elevated risk of PC.

REFERENCES

1. Siegel R, Ma J, Zou Z, et al. Cancer statistics, 2014. *CA Cancer J Clin*. 2014;64:9–29.
2. Yachida S, Jones S, Bozic I, et al. Distant metastasis occurs late during the genetic evolution of pancreatic cancer. *Nature*. 2010;467:1114–1117.
3. Turzhitsky V, Liu Y, Hasabou N, et al. Investigating population risk factors of pancreatic cancer by evaluation of optical markers in the duodenal mucosa. *Dis Markers*. 2008;25:313–321.
4. Liu Y, Brand RE, Turzhitsky V, et al. Optical markers in duodenal mucosa predict the presence of pancreatic cancer. *Clin Cancer Res*. 2007;13:4392–4399.
5. Matsubayashi H, Sato N, Brune K, et al. Age- and disease-related methylation of multiple genes in nonneoplastic duodenum and in duodenal juice. *Clin Cancer Res*. 2005;11:573–583.
6. Matsubayashi H, Canto M, Sato N, et al. DNA methylation alterations in the pancreatic juice of patients with suspected pancreatic disease. *Cancer Res*. 2006;66:1208–1217.
7. Roy HK, Turzhitsky V, Kim Y, et al. Association between rectal optical signatures and colonic neoplasia: potential applications for screening. *Cancer Res*. 2009;69:4476–4483.
8. Anti M, Marra G, Armelao F, et al. Rectal epithelial-cell proliferation patterns as predictors of adenomatous colorectal polyp recurrence. *Gut*. 1993;34:525–530.
9. Bernstein C, Bernstein H, Garewal H, et al. A bile acid-induced apoptosis assay for colon cancer risk and associated quality control studies. *Cancer Res*. 1999;59:2353–2357.
10. Steiling K, Ryan J, Brody JS, et al. The field of tissue injury in the lung and airway. *Cancer Prev Res (Phila)*. 2008;1:396–403.
11. Spira A, Beane JE, Shah V, et al. Airway epithelial gene expression in the diagnostic evaluation of smokers with suspect lung cancer. *Nat Med*. 2007;13:361–366.
12. Slaughter DP, Southwick HW, Smejkal W. Field cancerization in oral stratified squamous epithelium; clinical implications of multicentric origin. *Cancer*. 1953;6:963–968.
13. Farrell JJ, Zhang L, Zhou H, et al. Variations of oral microbiota are associated with pancreatic diseases including pancreatic cancer. *Gut*. 2012;61:582–588.
14. Kedia P, Gaidhane M, Kahaleh M. Technical advances in endoscopic ultrasound (EUS)-guided tissue acquisition for pancreatic cancers: how can we get the best results with eus-guided fine needle aspiration? *Clin Endosc*. 2013;46:552–562.

15. Radosevich AJ, Yi J, Rogers JD, et al. Structural length-scale sensitivities of reflectance measurements in continuous random media under the Born approximation. *Opt Lett*. 2012;37:5220–5222.
16. Radosevich AJ, Mutyal NN, Yi J, et al. Ultrastructural alterations in field carcinogenesis measured by enhanced backscattering spectroscopy. *J Biomed Opt*. 2013;18:097002. doi:10.1117/1.JBO.18.9.097002.
17. Stypula-Cyrus Y, Damania D, Kunte DP, et al. HDAC up-regulation in early colon field carcinogenesis is involved in cell tumorigenicity through regulation of chromatin structure. *PLoS One*. 2013;8:e64600.
18. Backman V, Roy HK. Advances in biophotonics detection of field carcinogenesis for colon cancer risk stratification. *J Cancer*. 2013;4:251–261.
19. Yi J, Radosevich AJ, Stypula-Cyrus Y, et al. Spatially resolved optical and ultrastructural properties of colorectal and pancreatic field carcinogenesis observed by inverse spectroscopic optical coherence tomography. *J Biomed Opt*. 2014;19:36013.
20. Mutyal NN, Radosevich A, Gould B, et al. A fiber optic probe design to measure depth-limited optical properties in-vivo with low-coherence enhanced backscattering (LEBS) spectroscopy. *Opt Express*. 2012;20:19643–19657.
21. Rogers JD, Radosevich AJ, Ji Y, et al. Modeling light scattering in tissue as continuous random media using a versatile refractive index correlation function. *IEEE Journal of Selected Topics in Quantum Electronics*. 2014;20:1–14.
22. Rogers JD, Capoglu IR, Backman V. Nonscalar elastic light scattering from continuous random media in the Born approximation. *Opt Lett*. 2009;34:1891–1893.
23. Ishimaru A. *Wave Propagation and Scattering in Random Media*. New York: IEEE Press-Oxford University Press; 1997.
24. Turzhitsky V, Radosevich A, Rogers JD, et al. A predictive model of backscattering at subdiffusion length scales. *Biomed Opt Express*. 2010;1:1034–1046.
25. Radosevich AJ, Mutyal NN, Turzhitsky V, et al. Measurement of the spatial backscattering impulse-response at short length scales with polarized enhanced backscattering. *Opt Lett*. 2011;36:4737–4739.
26. Radosevich AJ, Rogers JD, Turzhitsky V, et al. Polarized enhanced backscattering spectroscopy for characterization of biological tissues at subdiffusion length scales. *IEEE Journal of Selected Topics in Quantum Electronics*. 2012;18:1313–1325.
27. Kim YL, Liu Y, Turzhitsky VM, et al. Coherent backscattering spectroscopy. *Opt Lett*. 2004;29:1906–1908.
28. Rogers JD, Stoyneva V, Turzhitsky V, et al. Alternate formulation of enhanced backscattering as phase conjugation and diffraction: derivation and experimental observation. *Opt Exp*. 2011;19:11922–11931.
29. Turzhitsky V, Mutyal NN, Radosevich AJ, et al. Multiple scattering model for the penetration depth of low-coherence enhanced backscattering. *J Biomed Opt*. 2011;16:097006.
30. Cheong WF, Prahl SA, Welch AJ. A review of the optical-properties of biological tissues. *IEEE Journal of Selected Topics in Quantum Electronics*. 1990;26:2166–2185.
31. Turzhitsky V, Radosevich AJ, Rogers JD, et al. Measurement of optical scattering properties with low-coherence enhanced backscattering spectroscopy. *Opt Lett*. 2011;36:4737–4739.
32. Cherkezyan L, Stypula-Cyrus Y, Subramanian H, et al. Nanoscale changes in chromatin organization represent the initial steps of tumorigenesis: a transmission electron microscopy study. *BMC Cancer*. 2014;14:189.
33. Stypula-Cyrus Y, Mutyal NN, Dela Cruz M, et al. End-binding protein 1 (EB1) up-regulation is an early event in colorectal carcinogenesis. *FEBS Lett*. 2014;588:829–835.
34. Mutyal NN, Radosevich A, Tiwari AK, et al. Biological mechanisms underlying structural changes induced by colorectal field carcinogenesis measured with low-coherence enhanced backscattering (LEBS) spectroscopy. *PLoS One*. 2013;8:e57206.
35. Turzhitsky VM, Gomes AJ, Kim YL, et al. Measuring mucosal blood supply in vivo with a polarization-gating probe. *Appl Opt*. 2008;47:6046–6057.
36. Correa-Gallego C, Ferrone CR, Thayer SP, et al. Incidental pancreatic cysts: do we really know what we are watching? *Pancreatology*. 2010;10:144–150.